RSC Advances

PAPER

Cite this: *RSC Adv.*, 2019, **9**, 17791

High throughput metabolomics-proteomics investigation on metabolic phenotype changes in rats caused by *Radix Scrophulariae* using ultra-performance liquid chromatography with mass spectrometry†

Fang Lu,‡[a] Ning Zhang,‡[b] Tao Ye,‡[b] Hongwei Zhao,[a] Mu Pang[a] and Shu-min Liu*[ac]

Received 20th December 2018
Accepted 31st May 2019

DOI: 10.1039/c8ra10443c

rsc.li/rsc-advances

Radix Scrophulariae, a traditional Chinese herb, is used to treat various diseases, including H_2O_2-induced apoptosis in cardiomyocytes, HaCaT cells, hyperuricaemia, and depression. This study screened metabolites, proteins and common pathways to better understand both the therapeutic effects and side effects of this herb. *Methods*: Untargeted metabolomics based on UPLC-TOF-MS, coupled with proteomics based on nano-UPLC-Q-Exactive-MS/MS, were used to investigate the effects of *R. Scrophulariae* in rats. Fifty-one identified metabolites in urine samples and 76 modulated proteins in liver tissue were potential biomarkers for *R. Scrophulariae* treatment. The biomarkers and common pathways involved were steroid hormone biosynthesis, drug metabolism-cytochrome p450, drug metabolism-other enzymes, pentose and glucuronate interconversions, and starch and sucrose metabolism. Some biomarkers were beneficial for treating diseases such as cancer, tuberculosis and isovaleric acidaemia, while other biomarkers caused side effects. Metabolomic and proteomic analyses of *R. Scrophulariae*-treated rats provided valuable information on the biological safety and efficacy of using *R. Scrophulariae* clinically.

1 Introduction

Radix Scrophulariae, the dried root of *Scrophularia ningpoensis* Hemsl., belongs to the Scrophulariaceae family and has been used in TCM for thousands of years. Per the Pharmacopoeia of the People's Republic of China (2015 Edition), the species' traditional functions include treating febrile diseases, constipation, hot eyes, pharyngalgia, diphtheria, and scrofula. Modern pharmacological research has shown that *R. Scrophulariae* inhibits ventricular remodelling,[1–4] hypoxia-induced microglial activation and neurotoxicity,[5] hypertension and attenuating arteriosclerosis,[6] proliferation, apoptosis induction in cancer cell lines,[7] and antioxidative activity.[8] TCMs are administered orally; therefore, their metabolites and proteins are disturbed when the blood circulation contacts the target organs. TCMs are therapeutic but also have side effects. For clinical use, the safety and effectiveness of TCMs are most important. These fundamental rules will guide exploitation of the biological effects of *R. Scrophulariae*.

The integrated metabolomics and proteomics based on mass spectrometry represents an innovative approach to characterize molecule fingerprints related to the function.[9–13] Here, metabolomics coupled with iTRAQ-based proteome profile analysis of these biological effects were employed to screen the key metabolites from urine samples and liver proteins by UPLC-TOF-MS and nano-UPLC-Q-Exactive-MS/MS, respectively.

2 Materials and methods

2.1 Plant material and extract preparation

The root of *Scrophularia ningpoensis* Hemsl. is a natural medicine. *R. Scrophulariae* was acquired from the Heilongjiang Province Drug Company (Harbin, PR China). The voucher specimen (hlj-20120623012) for the herb was authenticated by Prof. Zhenyue Wang of the Department of Resources and Development of TCM at Heilongjiang University of Traditional Chinese Medicine, meeting the standards of the Pharmacopoeia of the People's Republic of China (2015 edition), page 117.

Fatty oil of *R. Scrophulariae* was prepared with the 1 kg crude drug, which was extracted twice with 0.6 l petroleum ether for

[a]*Chinese Medicine Toxicological Laboratory, Heilongjiang University of Chinese Medicine, Harbin, P. R. China*

[b]*Fist Affiliated Hospital of Guiyang University of Traditional Chinese Medicine, Guizhou, Guiyang, P. R. China*

[c]*Drug Safety Evaluation Center, Heilongjiang University of Chinese Medicine, He Ping Road 24, Harbin 150040, P. R. China. E-mail: keji-liu@163.com; Fax: +86 45182193278; Tel: +86 45182193278*

† Electronic supplementary information (ESI) available. See DOI: 10.1039/c8ra10443c

‡ These authors contributed equally to this work.

12 h each. The two portions were mixed and concentrated into cream, then the drug residue was freeze-dried and extracted twice with 10 and 8 l distilled water (DW) for 1.5 h each, respectively. The two portions were mixed and concentrated into cream, comprising the aqueous extract of *R. Scrophulariae*. The eluates were freeze-dried to make extracts with a yield of 50.7%.

2.2 Rats and treatments

Healthy male Sprague-Dawley rats, weighing 200 ± 20 g each, were purchased from Liaoning Changsheng Biotechnology Co., Ltd. (PR China) (Animal Certificate No: SCXK [Liao] 2015-0001). Rats were fed a standard diet with free access to water and housed 1 per metabolic cage at a temperature of 21–23 °C and humidity at 40–50% in controlled rooms with a 12 h/12 h light/dark cycle. This study was conducted in strict accordance with the recommendations in the Guide for the Care and Use of Laboratory Animals of the National Institutes of Health. The protocol was subject to approval by the Committee on the Ethics of Animal Experiments of the College of Pharmacy of Heilongjiang University of Chinese Medicine.

After acclimation for 1 week, 20 rats were randomly divided into two groups, the control group and the water decoction of *R. Scrophulariae* group ($n = 10$ per group). Rats in the *R. Scrophulariae* group received decoction of *R. Scrophulariae* (1350 mg crude drug per kg, i.g.) once daily for 15 consecutive days, and rats in the control group received the same volume of 0.9% saline once daily for 15 days.

2.3 Sample collection and preparation

For the metabolomic analysis, urine was collected from all rats in each group on days 0, 1, 3, 5, 7, 9, 11, 13 and 15. Urine was centrifuged twice at 10 000 g for 10 min at 4 °C to remove the solid residue. Supernatants were transferred to a 1.5 ml polypropylene tube and filtered through a syringe filter (0.22 μm). Two μl of the supernatant was injected into the UPLC/TOF-MS for analysis.

For the proteomic analysis, rats were anaesthetized with 1% sodium pentobarbital anaesthesia (0.15 ml/100 g), and liver samples were obtained. Each group was analysed in triplicate ($n = 10$ per group) and then mixed into 3 mixed samples and stored at −80 °C. After thawing, 100 μl of STD buffer (4% SDS [161-0302, Bio-Rad], 1 mM DTT [161-0404 Bio-Rad], 150 mM Tris–HCl pH 8.0) per 20 μg sample was added and homogenized with a tissue homogenizer for 5 min in a boiling water bath. The mix was ultrasonicated (80 W) for 10 s and intermittently for 15 s ten times, then incubated in boiling water for 5 min and centrifuged at 14 000 g for 10 min. The supernatant was removed and subjected to 12.5% SDS-PAGE electrophoresis.

2.4 Metabolic profiling platform

2.4.1 LC-MS analysis. Metabolomic analysis was performed on a Waters ACQUITY UPLC system coupled with time-of-flight mass spectrometry. Chromatography was performed using an ACQUITY BEH C18 chromatography column (2.1 mm × 100 mm, 1.7 μm). Column and sample temperatures were set at 40.0 °C and 4.0 °C, respectively. The gradient mobile phase conditions consisted of solvent A (0.05% FA-ACN) and solvent B (0.05% FA-H_2O). The urine sample gradient was as follows: 0–8 min, 2.0–40% A; 8–10 min, 40.0–98% A; 10–13 min, 98.0–100.0% A; 13–14 min, 100.0–2% A; 14–17 min, 2% A. The flow rate was 0.400 ml min^{-1}. To guarantee system stability and repeatability, quality control (QC) samples were inserted every 10 samples, which was urine, and not a single sample collected in the experiment, but a mixed one of 10 samples per group taken from 100 to 200 μl of each. MS parameters were established as follows. Mass range was from 100 to 1500 in the full scan mode. Desolvation temperature and source temperature were set at 350.0 °C and 110.0 °C, respectively. Cone gas flow and desolvation gas flow rate were maintained at 20.0 l h^{-1} and 750.0 l h^{-1}, respectively. Capillary voltage was set at 1300.0 V in the positive ions (ESI^+) mode and 1500.0 V in the negative ions (ESI^-) mode. Sample cone voltage was set to 60.0 V (ESI^+) and 70.0 V (ESI^-). Ion energy voltage was set to 35.0 V (ESI^+) and 34.0 V (ESI^-). Scan duration time and inter-scan delay were set to 0.200 s and 0.010 s, respectively. Leucine-enkephalin was the lock-mass compound (556.2771 $[M + H]^+$ and 554.2615 $[M - H]^-$).

2.4.2 Multivariate data analysis. Raw data acquired by UPLC-TOF-MS were exported to the Progenesis QI v2.3 (Nonlinear Dynamics, Waters Company) workstation for peak alignment, peak picking, and deconvolution. The data matrix (Rt-*m*/*z*, normalised abundance, and adducts) were exported to Ezinfo 3.0.3.0 software for principal component analysis (PCA), partial least squares discriminant analysis (PLS-DA) and orthogonal partial least squares discriminant analysis (OPLS-DA). We first performed a non-discriminatory PCA analysis. If the identified metabolites were Scrophulariaceae components, they would be removed from the original data and then analyzed by PCA. Of these analyses, 2D or 3D-PCA score plots reflected the clustering degree of each group. To analyse the urine metabolic profiles between the experimental and control groups, OPLS-DA score plots were constructed to obtain the VIP-plot, *S*-plot and loading plot. Variables farther from the origin contributed significantly in these plots. Using $P < 0.05$ and variables important for the projection (VIP) value > 1 as the standards, potential biomarkers were selected and compared with HMDB (http://www.hmdb.ca/) and progenesis metascope. Metabolic pathway analysis was performed using KEGG (http://www.kegg.jp/).

2.5 Proteomics analysis

The electrophoretic conditions were kept at a constant current for 90 min. The 300 μg samples were filter-aided for sample preparation (FASP). Eighty μg peptide samples from each group were labelled per the iTRAQ Reagent-8plex Multiplex Kit (AB SCIEX) instructions. Strong cation exchange (SCX) chromatography was performed on an AKTA Purifier 100 (GE Healthcare) coupled with a polysulfoethyl 4.6 × 100 mm column (5 μm, 200 Å) (PolyLC, Inc., Maryland, U.S.A.). Buffers were composed of buffer A (10 mM KH_2PO_4 pH 3.0, 25% ACN) and buffer B (10 mM KH_2PO_4 pH 3.0, 500 mM KCl, 25% ACN) with a flow rate of 1000

μl min^{-1}. SCX gradient was set as follows: 0–25.01 min, 100% A; 25.01–32.00 min, 100–90% A; 32.01–42.00 min, 90–80% A; 42.01–47.00 min, 80–55% A; 47.01–52 min, 55–0% A; 52–60 min, 0% A; 60–60.01 min, 0–100% A; 60.01–75.00 min, 100% A.

Samples were separated by an automated Easy-nLC system coupled with a Q-Exactive spectrometer (Thermo Finnigan, USA). Buffer was composed of solution A (water containing 0.1% FA) and solution B (84% ACN containing 0.1% FA). Protein samples were performed on a thermo scientific EASY C18 column (2 cm × 100 μm, 5 μm), and separated on a thermo scientific EASY C18 column (75 μm × 100 mm, 3 μm). The flow rate was 300 nL min^{-1}. The gradient elution procedure was as follows: 0–55 min, 0–40% B; 55–58 min, 40–100% B; 58–60 min, 100% B. The scan range was set to 300–1800 *m*/*z* in positive ion mode. The AGC target was set to 3 × 10^6. The maximum injection time was 10 ms. The normalized collision energy was 30 eV. The underfill ratio was 0.1%. The mass resolution for full MS and dd-MS^2 were 70 000 and 17 500, respectively.

2.5.1 Data processing. Raw peptide files were searched with the Mascot 2.2 and Proteome Discoverer 1.4 (thermo) and a database of uniprot_rat_35830_20160326 fasta. Mascot search parameters were set as follows: fixed modifications were carbamidomethyl (C), iTRAQ8plex (N-term), iTRAQ8plex (K) and variable modification was oxidation (M); enzyme was set to trypsin; mass values were set to monoisotopic; max missed cleavages were set to 2; peptide mass tolerance was ± 20 ppm; fragment mass tolerance was 0.1 Da; and the database pattern was a decoy. Heatmaps were constructed by MetaboAnalyst 3.0 online (http://www.metaboanalyst.ca/). Protein identities were linked to the following databases: Quick GO (Gene Ontology Analysis), KEGG Pathway (Pathway Analysis) and STRING (Protein–Protein Interaction Analysis) for downstream analysis.

3 Results and discussion

3.1 Metabolomic profile analysis

In OPLS-DA, urine samples from the *R. Scrophulariae* group were separated from the control group, revealing that the rats' metabolic profiles changed after *R. Scrophulariae* treatment (Fig. 1A). VIP-plot and *S*-plot for evaluating contribution degree are shown in Fig. 1B and C. Fifty-one differential metabolites were consistent with $P < 0.05$, VIP > 1, and maximum fold change > 1 after being retrieved and matched by Metlin, HMDB and KEGG (Fig. 2A and Table 1).Endogenous small metabolites were classified using the HMDB database, and 26% were classified as amino acids, peptides, and analogues, 23% were benzenoids, and 19% were lipids (Fig. 2B). For biofunction, 16% were subgrouped into waste products, and cell signalling, fuel and energy storage, fuel or energy source and membrane integrity/stability accounted for 15% each (Fig. 2C). These metabolites were primarily located in the cytoplasm, membrane, extracellular matrix and mitochondria (Fig. 2D).

Pathway analysis was performed using MetaboAnalyst 3.0 software, revealing that endogenous small molecule metabolites were concentrated in the metabolisms of nicotinate and nicotinamide, phenylalanine, tyrosine and pyrimidine, and in phenylalanine, tyrosine and tryptophan biosynthesis (Fig. 2E).

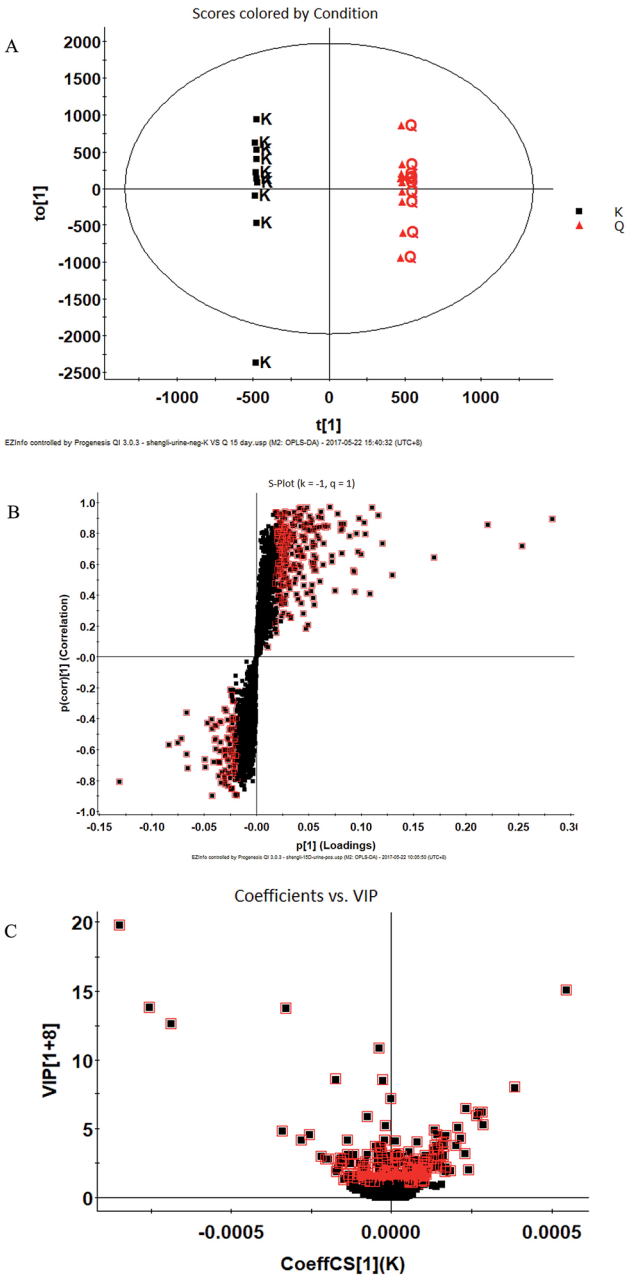

Fig. 1 Urine sample score plots for the *R. Scrophulariae* and control groups. (A) OPLS-DA score plots for the urine samples between the two groups, K represents the control, and Q represents the *R. Scrophulariae* group; (B) *S*-plots of urine samples between two groups; (C) VIP-plots of urine. Samples between the two groups.

3.2 Liver proteomic profile

Seventy-six significant proteins were selected by $P < 0.05$ and ratio >1.2 or <0.833 and are listed in Table 2. Compared with the control, expression levels of 31 proteins were down-regulated, while 45 were up-regulated. Seventy-six changed proteins were further enriched using the Bonferroni correction for multiple testing ($P < 0.05$) through GO analysis, and the GO terms for fold enrichment are shown in Fig. 3A. Seventy-six proteins participated in single-organism metabolic processes. These proteins were primarily involved in catalytic and electron carrier

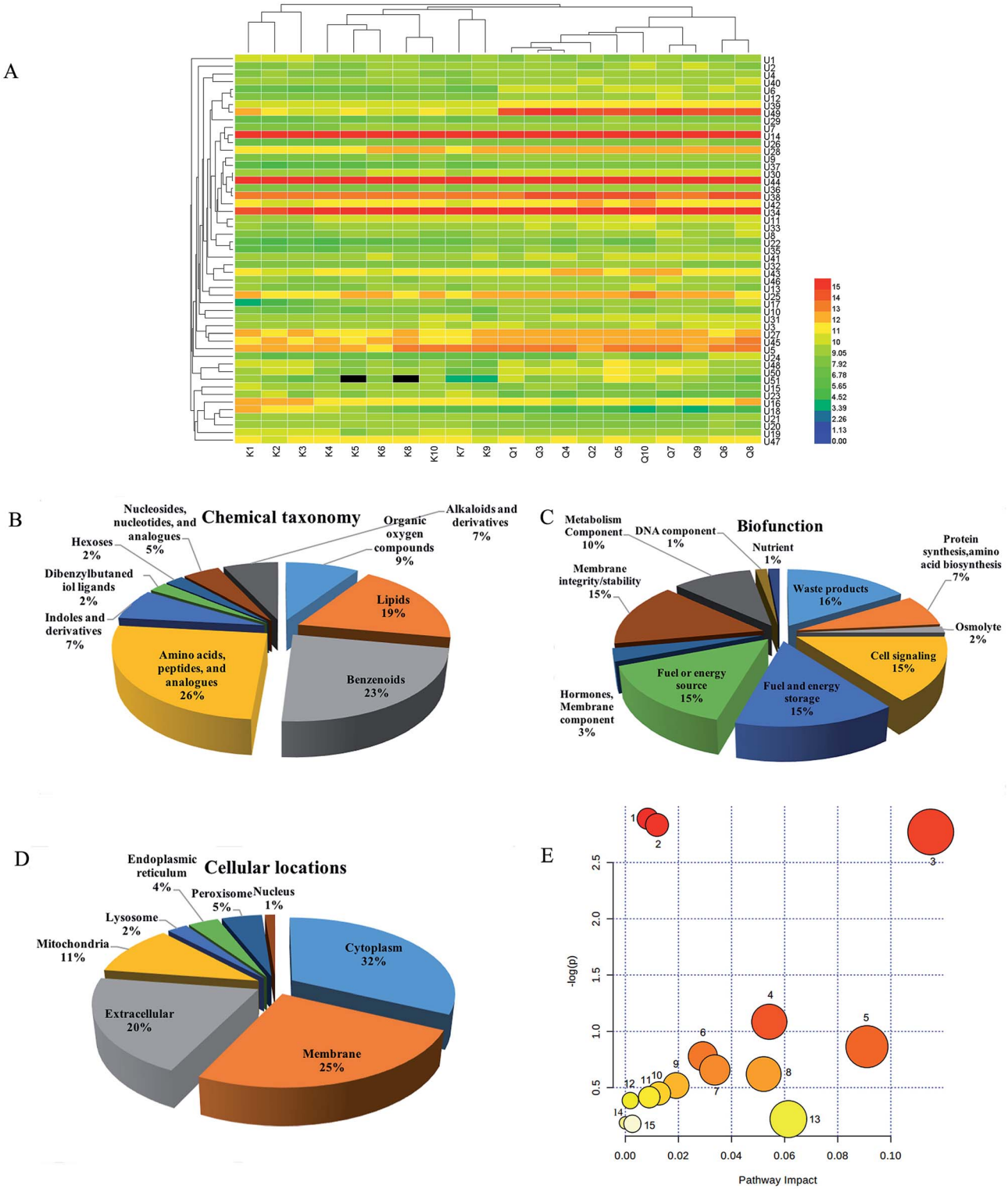

Fig. 2 Metabolites expression profiling and pathway analysis of the *R. Scrophulariae* and control groups. (A) Heatmap of urine metabolites between the two groups. (B–D) Classification of potential biomarkers related to *R. Scrophulariae* in urine samples by chemical taxonomy, biofunction and cellular components based on HMDB annotations. (E) Topological mapping of potential biomarkers based on METPA analysis. (1) Nicotinate and nicotinamide metabolism; (2) phenylalanine metabolism; (3) tyrosine metabolism; (4) pyrimidine metabolism; (5) phenylalanine, tyrosine and tryptophan biosynthesis; (6) arginine and proline metabolism; (7), ubiquinone and other terpenoid-quinone biosynthesis; (8), drug metabolism – other enzymes; (9) steroid hormone biosynthesis; (10) starch and sucrose metabolism; (11) pentose and glucuronate interconversions; (12) cysteine and methionine metabolism; (13), tryptophan metabolism; (14) drug metabolism – cytochrome P450; (15) amino sugar and nucleotide sugar metabolism.

Table 1 Significant differential metabolites produced in the urine after the intervention of Scrophulariaceae in normal rats[a]

No.	Rt-*m*/*z*	HMDB ID	Ions mode	KEGG	Formula	Metabolites	VIP value	Trends (Q/K)	Anova (*p*)	*q* value	Max fold change
U1	10.70_207.1034	HMDB11603	pos	C16453	$C_{10}H_{13}N_3O_2$	4-(Methylnitrosamino)-1-(3-pyridyl)-1-butanone	1.1366	Down*	0.0171	0.0450	1.5678
U2	4.45_202.1225	HMDB00792	pos	C08277	$C_{10}H_{18}O_4$	Sebacic acid	1.9215	Up*	0.0145	0.0402	1.4905
U3	1.39_153.0816	HMDB04825	pos	C04227	$C_8H_{11}NO_2$	*p*-Octopamine	1.1147	Up**	0.0029	0.0123	1.2995
U4	2.56_160.1227	HMDB02038	pos	C02728	$C_7H_{16}N_2O_2$	N(6)-Methyllysine	1.0838	Up**	0.0000	0.0009	1.3617
U5	2.56_143.0966	HMDB04827	pos	C10172	$C_7H_{13}NO2$	Proline betaine	3.5748	Up*	0.0109	0.0325	1.3654
U6	3.50_275.1305	HMDB13209	pos	C00806	$C_{14}H_{17}N_3O_3$	Alanyltryptophan	2.5677	Up**	0.0000	0.0000	5.6666
U7	3.96_286.1515	HMDB00343	pos	C05298	$C_{18}H_{22}O_3$	2-Hydroxyestrone	1.0815	Up**	0.0028	0.0120	1.4051
U8	0.93_172.0633	HMDB01138	pos	C00624	$C_7H_{11}NO_5$	N-Acetylglutamic acid	1.4061	Up**	0.0000	0.0007	1.5997
U9	0.96_202.1108	HMDB00216	pos	C00547	$C_8H_{11}NO_3$	Norepinephrine	1.3643	Up**	0.0000	0.0005	1.5478
U10	0.97_284.1007	HMDB00472	pos	C01017	$C_{11}H_{12}N_2O_3$	5-Hydroxy-L-tryptophan	1.1434	Up**	0.0016	0.0080	1.8401
U11	1.81_267.1359	HMDB05056	pos	C18166	$C_{18}H_{22}O_4$	Enterodiol	1.7389	Up**	0.0004	0.0031	1.4417
U12	1.84_144.0672	HMDB01514	pos	C00329	$C_6H_{13}NO_5$	Glucosamine	1.9440	Up**	0.0000	0.0000	2.5749
U13	2.23_275.1260	HMDB00273	pos	C00214	$C_{10}H_{14}N_2O_5$	Thymidine	1.0469	Up**	0.0022	0.0103	1.4222
U14	2.31_297.1462	HMDB06344	pos	C04148	$C_{13}H_{16}N_2O_4$	Alpha-N-phenylacetyl-L-glutamine	13.5022	Up**	0.0009	0.0055	1.4501
U15	2.92_267.1004	HMDB00933	pos	C16308	$C_{12}H_{20}O_4$	Traumatic acid	1.2758	Up**	0.0000	0.0008	2.1394
U16	4.24_254.1154	HMDB41959	pos	C11785	$C_{16}H_{17}NO_3$	Normorphine	2.1217	Down*	0.0388	0.0802	1.5050
U17	10.65_190.0521	HMDB01553	pos	C01180	$C_5H_8O_3S$	2-Oxo-4-methylthiobutanoic acid	1.3511	Up*	0.0287	0.0664	1.7704
U18	10.09_151.0469	HMDB02091	pos	C03033	$C_{11}H_{18}O_8$	Isovalerylglucuronide	2.2095	Down**	0.0001	0.0013	36.6655
U19	6.49_316.1969	HMDB00306	pos	C00483	$C_8H_{11}NO$	Tyramine	1.0905	Down*	0.0350	0.0748	1.3971
U20	5.54_246.1721	HMDB02176	pos	C18319	$C_5H_{10}O_2$	Ethylmethylacetic acid	1.1394	Down**	0.0009	0.0055	1.5188
U21	5.35_278.1073	HMDB10328	pos	C03033	$C_{14}H_{19}NO_7$	Tyramine glucuronide	1.0563	Down**	0.0015	0.0080	1.4124
U22	4.79_158.0630	HMDB00821	pos	C05598	$C_{10}H_{11}NO_3$	Phenylacetylglycine	1.2436	Up**	0.0000	0.0008	3.3653
U23	4.33_348.1204	HMDB01476	pos	C00632	$C_7H_7NO_3$	3-Hydroxyanthranilic acid	1.7225	Down**	0.0003	0.0027	3.1281
U24	3.36_153.0933	HMDB00784	pos	C08261	$C_9H_{16}O_4$	Azelaic acid	1.1179	Up*	0.0142	0.0398	2.6331
U25	2.73_245.1513	HMDB00201	pos	C02571	$C_9H_{17}NO_4$	L-Acetylcarnitine	2.8023	Up**	0.0090	0.0282	1.4032
U26	2.62_197.0838	HMDB02035	pos	C00811	$C_9H_8O_3$	4-Hydroxycinnamic acid	1.0570	Up**	0.0001	0.0012	1.6887
U27	2.49_230.1422	HMDB04063	pos	C05588	$C_{10}H_{15}NO_3$	Metanephrine	1.8485	Up*	0.0144	0.0400	1.1881
U28	2.45_243.1353	HMDB13248	pos	C03343	$C_{16}H_{22}O_4$	Monoethylhexyl phthalic acid	2.7083	Up**	0.0007	0.0048	1.3543
U29	2.27_200.0756	HMDB00462	pos	C01551	$C_4H_6N_4O_3$	Allantoin	1.1143	Up**	0.0000	0.0002	1.8271
U30	2.18_261.0885	HMDB00181	pos	C00355	$C_9H_{11}NO_4$	L-Dopa	2.0865	Up**	0.0000	0.0002	1.5815
U31	2.05_413.1250	HMDB10334	pos	C03033	$C_{22}H_{22}O_9$	Ketoprofen glucuronide	1.1382	Up**	0.0084	0.0268	1.3105
U32	1.68_255.0778	HMDB01858	pos	C01468	C_7H_8O	*p*-Cresol	1.0839	Up**	0.0001	0.0011	1.5645
U33	1.65_265.1570	HMDB00010	pos	C05299	$C_{19}H_{24}O_3$	2-Methoxyestrone	1.3779	Up**	0.0006	0.0040	1.5384
U34	1.40_204.1350	HMDB00450	pos	C16741	$C_6H_{14}N_2O_3$	5-Hydroxylysine	11.9554	Up**	0.0000	0.0003	1.5922
U35	1.34_173.0461	HMDB12710	pos	C00944	$C_7H_{10}O_6$	3-Dehydroquinate	1.3519	Up**	0.0012	0.0069	2.1674
U36	1.30_259.1671	HMDB00824	pos	C03017	$C_{10}H_{19}NO_4$	Propionylcarnitine	1.4708	Up**	0.0021	0.0100	1.5050
U37	1.22_215.1049	HMDB32049	pos	C06354	$C_{13}H_{10}O$	Benzophenone	1.3260	Up**	0.0000	0.0003	2.9951
U38	1.22_166.0736	HMDB02303	pos	C00580	C_2H_6S	Dimethylsulfide	5.9549	Up**	0.0000	0.0001	1.4267
U39	1.20_158.0904	HMDB00904	pos	C00327	$C_6H_{13}N_3O_3$	Citrulline	2.6437	Up**	0.0000	0.0001	1.7277
U40	1.05_168.0684	HMDB00742	pos	C05330	$C_4H_9NO_2S$	Homocysteine	1.0606	Up**	0.0028	0.0122	1.3436
U41	0.95_261.1481	HMDB13835	pos	C15205	$C_{16}H_{22}O_4$	Diisobutyl phthalate	1.1423	Up**	0.0014	0.0076	1.2734
U42	0.90_269.1267	HMDB00014	pos	C00881	$C_9H_{13}N_3O_4$	Deoxycytidine	3.0487	Up**	0.0000	0.0001	1.5761
U43	0.87_227.0455	HMDB01890	pos	C06809	$C_5H_9NO_3S$	Acetylcysteine	3.1726	Up**	0.0001	0.0012	1.6787
U44	0.80_212.1014	HMDB41821	pos	C07585	$C_8H_9N_3O_2$	Acetylisoniazid	14.5218	Up**	0.0000	0.0003	1.6217
U45	0.74_144.1041	HMDB01010	pos	C00745	$C_{10}H_{13}N_2$	Nicotine imine	2.8013	Up**	0.0048	0.0179	1.3663
U46	0.68_176.0135	HMDB00875	pos	C01004	$C_7H_7NO_2$	Trigonelline	1.2566	Up**	0.0008	0.0049	1.4882
U47	7.86_253.1075	HMDB02004	neg	C08309	$C_{13}H_{18}N_2O$	5-Methoxydimethyltryptamine	1.4738	Down*	0.0235	0.5348	1.3094
U48	4.02_290.0707	HMDB00855	neg	C03150	$C_{11}H_{15}N_2O_5$	Nicotinamide riboside	1.2816	Up*	0.0252	0.5368	1.6344
U49	3.72_247.0284	HMDB04983	neg	C11142	$C_2H_6O_2S$	Dimethyl sulfone	13.8303	Up**	0.0000	0.0000	12.5966
U50	1.72_238.0757	HMDB13318	neg	C00977	$C_{11}H_{13}N_3O$	Tryptophanamide	1.6212	Up*	0.0113	0.4388	1.8896
U51	1.72_483.1785	HMDB10317	neg	C03033	$C_{24}H_{32}O_8$	17-Beta-estradiol glucuronide	1.3788	Up*	0.0194	0.5261	2.7223

[a] Compared with control group, $*p < 0.05$,$**p < 0.01$. U represents urine. K represents control group, Q represents *R. Scrophulariae* group.

activities and were mainly located in the organelles. It suggested that the function of *R. Scrophulariae* is related to a complicated biological process. Twelve significant KEGG pathways were selected by $-\log p$ value > 2 and are shown in Fig. 3B. The protein–protein interaction (PPI) network was analysed by the publicly available programme STRING (http://string-db.org/). STRING is a database of known and predicted protein interactions. PPI nodes such as COX2, ND2, Cyp17a1, Hsd17b2, Mgst3, Ugt2b, Cyp2c13, RT1-CE1, Mn1 and Psmb8 might play key roles in the functional mechanism of *R. Scrophulariae* (Fig. 3C).

Table 2 Significantly different proteins produced in the liver after the intervention of Scrophulariaceae in normal rats (difference multiple >1.2 or <0.8)[a]

No.	Accession	Gene name	Description	Average ratio Q/K	Trends Q/K	*P* value
L1	Q6MG32	RT1-CE12	RT1 class I, CE12	0.4685	Down**	0.0002
L2	Q63042	Gfer	FAD-linked sulfhydryl oxidase ALR	0.5479	Down**	0.0022
L3	A0A0G2JSK1	Serpina3c	Protein Serpina3c	0.5502	Down**	0.0001
L4	P35286	Rab13	Ras-related protein Rab-13	0.6139	Down*	0.0458
L5	M0R9Q1	Rbm14	Protein Rbm14	0.6297	Down**	0.0005
L6	Q4VBH1	Ighg	Ighg protein	0.6415	Down**	0.0004
L7	A0A023IKI3	Psmb8	Proteasome subunit beta type	0.6454	Down**	0.0047
L8	A0A0G2JX10	Anks3	Ankyrin repeat and SAM domain-containing protein 3	0.6764	Down**	0.0022
L9	P70473	Amacr	Alpha-methylacyl-CoA racemase	0.6981	Down**	0.0003
L10	M0RAJ5	Prr14l	Protein Prr14l	0.7129	Down**	0.0069
L11	Q6P756	Necap2	Adaptin ear-binding coat-associated protein 2	0.7407	Down*	0.0151
L12	Q80W92	Vac14	Protein VAC14 homolog	0.7429	Down*	0.0338
L13	A0A097PE04	COX2	Cytochrome *c* oxidase subunit 2	0.7470	Down**	0.0005
L14	Q5RK24	Pmvk	Phosphomevalonate kinase	0.7552	Down**	0.0019
L15	Q99MS0	Sec14l2	SEC14-like protein 2	0.7571	Down**	0.0009
L16	E9PU17	Abca17	ATP-binding cassette sub-family A member 17	0.7599	Down*	0.0271
L17	F1LM99	Phf12	PHD finger protein 12	0.7733	Down**	0.0045
L18	A0A0G2JVQ0	Rnf111	Protein Rnf111	0.7744	Down*	0.0444
L19	D3ZTW7	Atpaf2	ATP synthase mitochondrial F1 complex assembly factor 2 (predicted), isoform CRA_c	0.7886	Down**	0.0012
L20	P43424	Galt	Galactose-1-phosphate uridylyltransferase	0.7907	Down**	0.0076
L21	A0A0G2JV37	LOC100910040	Carboxylic ester hydrolase	0.7914	Down*	0.0305
L22	P49889	Ste	Estrogen sulfotransferase, isoform 3	0.7941	Down**	0.0050
L23	Q6AYW2	Pah	Phenylalanine hydroxylase	0.7994	Down**	0.0088
L24	P55006	Rdh7	Retinol dehydrogenase 7	0.8006	Down**	0.0001
L25	P0C5E9	Crygs	Beta-crystallin S	0.8026	Down**	0.0075
L26	A0A0G2KA12	Kif1b	Kinesin-like protein KIF1B	0.8111	Down*	0.0244
L27	F1LRB8	Mat2a	*S*-Adenosylmethionine synthase	0.8113	Down**	0.0057
L28	B2GV29	Trmt13	Ccdc76 protein	0.8139	Down**	0.0016
L29	Q4QR81	Rbms2	Protein Rbms2	0.8203	Down*	0.0224
L30	D4AAP6	Mn1	Protein Mn1	0.8215	Down**	0.0016
L31	D4AB73	Sprtn	Putative uncharacterized protein RGD1559496_predicted	0.8298	Down*	0.0177
L32	Q5XHZ8	Cog3	Component of oligomeric golgi complex 3	1.2021	Up**	0.0011
L33	P00502	Gsta1	Glutathione *S*-transferase alpha-1	1.2046	Up**	0.0000
L34	P19488	Ugt2b37	UDP-glucuronosyltransferase 2B37	1.2057	Up**	0.0045
L35	Q6AXQ0	Sae1	SUMO-activating enzyme subunit 1	1.2057	Up*	0.0347
L36	F1LNM4	LOC103689965	Complement C4 (fragment)	1.2075	Up**	0.0039
L37	F1LU27	Focad	Protein Focad	1.2138	Up*	0.0489
L38	Q32PY9	Idnk	Probable gluconokinase	1.2167	Up**	0.0068
L39	G3V647	Pdxk	Pyridoxal kinase	1.2222	Up**	0.0010
L40	P05545	Serpina3k	Serine protease inhibitor A3K	1.2300	Up**	0.0100
L41	G3V9N9	Man1a1	Alpha-1,2-mannosidase	1.2303	Up**	0.0040
L42	Q566C7	Nudt3	Diphosphoinositol polyphosphate phosphohydrolase 1	1.2349	Up**	0.0001
L43	F1LN59	Eif4g2	Protein Eif4g2	1.2408	Up**	0.0084
L44	D4A284	Nell1	NEL-like 1 (chicken), isoform CRA_a	1.2417	Up*	0.0180
L45	D3ZNJ5	Inmt	Protein Inmt	1.2494	Up**	0.0027
L46	A0A0G2JU41	Dyrk4	Protein Dyrk4	1.2503	Up**	0.0015
L47	D4ADS4	Mgst3	Protein Mgst3	1.2523	Up**	0.0007
L48	A0A0G2JSR8	Cyp17a1	Cytochrome P450, family 17, subfamily a, polypeptide 1	1.2576	Up**	0.0077
L49	A2VCW9	Aass	Alpha-aminoadipic semialdehyde synthase, mitochondrial	1.2637	Up**	0.0000
L50	F1M7N8	Ugt2b37	UDP-glucuronosyltransferase	1.2647	Up**	0.0010
L51	P38659	Pdia4	Protein disulfide-isomerase A4	1.2670	Up**	0.0018
L52	Q6AXR4	Hexb	Beta-hexosaminidase subunit beta	1.2712	Up**	0.0021
L53	D4A3E8	Mrps27	Mitochondrial ribosomal protein S27 (predicted), isoform CRA_b	1.2733	Up*	0.0453
L54	D3ZES7	Plxna4	Protein Plxna4	1.2853	Up**	0.0001
L55	P05183	Cyp3a2	Cytochrome P450 3A2	1.3085	Up**	0.0002
L56	Q5XIG0	Nudt9	ADP-ribose pyrophosphatase, mitochondrial	1.3121	Up**	0.0001
L57	Q920L7	Elovl5	Elongation of very long chain fatty acids protein 5	1.3239	Up**	0.0021
L58	P08290	Asgr2	Asialoglycoprotein receptor 2	1.3334	Up*	0.0127

Table 2 (*Contd.*)

No.	Accession	Gene name	Description	Average ratio Q/K	Trends Q/K	*P* value
L59	A0A023IM45	Psmb8	Proteasome subunit beta type	1.3358	Up**	0.0020
L60	Q62730	Hsd17b2	Estradiol 17-beta-dehydrogenase 2	1.3607	Up**	0.0000
L61	Q31256	N/A	MHC class I RT1.Au heavy chain	1.3778	Up**	0.0003
L62	A0A0A1G491	ND2	NADH-ubiquinone oxidoreductase chain 2	1.3851	Up*	0.0195
L63	P20814	Cyp2c13	Cytochrome P450 2C13, male-specific	1.4111	Up**	0.0000
L64	F1LMF4	Fat3	Protocadherin fat 3	1.4253	Up**	0.0060
L65	Q4V797	RGD1309362	Interferon-gamma-inducible GTPase Ifgga1 protein	1.4272	Up**	0.0000
L66	P50169	Rdh3	Retinol dehydrogenase 3	1.4563	Up**	0.0000
L67	A0A0G2K222	N/A	Uncharacterized protein	1.5162	Up	0.0272
L68	Q5UAJ6	COX2	Cytochrome *c* oxidase subunit 2	1.5316	Up**	0.0001
L69	M0RC39	Olr796	Olfactory receptor	1.5880	Up*	0.0484
L70	D3ZMQ0	Mga	Protein Mga	1.6374	Up*	0.0312
L71	Q6T5E9	Ugt1a6	UDP-glucuronosyltransferase	1.7279	Up**	0.0003
L72	A1XF83	Ugt2b	UDP-glucuronosyltransferase	1.8256	Up**	0.0001
L73	D3ZXC8	Ebpl	Emopamil binding protein-like (predicted), isoform CRA_a	1.8324	Up**	0.0018
L74	F1LM22	Ugt2b	UDP-glucuronosyltransferase	1.8894	Up**	0.0000
L75	Q63002	Igf2r	Mannose 6-phosphate/insulin-like growth factor II receptor	2.1130	Up**	0.0080
L76	Q5BK88	Amacr	Alpha-methylacyl-CoA racemase	2.5845	Up**	0.0001

[a] Compared with control group, $*p < 0.05$,$**p < 0.01$. L represents liver. K represents control group, Q represents *R. Scrophulariae* group.

3.3 Common pathways analysis

The common KEGG pathways between proteins and metabolism were steroid hormone biosynthesis, drug metabolism – cytochrome p450, drug metabolism – other enzymes, pentose and glucuronate interconversions, and starch and sucrose metabolism. Among them, the proteins engaged in steroid hormone biosynthesis were Ste, Ugt2b37, Cyp17a1, Cyp3a2, Hsd17b2, Cyp2c13, Ugt1a6 and Ugt2b, and the metabolites were 2-hydroxyestrone and 2-methoxyestrone. The proteins related to drug metabolism – cytochrome p450 were Gsta1, Ugt2b37, mgst3, Ugt1a6 and Ugt2b, and the metabolite was normorphine. The proteins participating in drug metabolism – other enzymes were carboxylic ester hydrolase, Ugt2b37, Ugt1a6 and Ugt2b. The proteins associated with the two pathways were Ugt2b37, Ugt1a6 and Ugt2b, and the metabolites were isovalerylglucuronide and tyramine glucuronide.

R. Scrophulariae enhanced 2-hydroxyestrone and 2-methoxyestrone expression in the urine. The direct precursor of 2-methoxyestrone is 2-hydroxyestrone, while the direct precursor of the latter is estrone. Ste levels decreased in the liver. Ste catalyses the transfer reaction from estrone to estrone sulfate and adenosine 3′,5′-diphosphate (PAP).[14] PAP accumulation is toxic to several cellular systems.[15] In addition, *R. Scrophulariae* enhanced the levels of Ugt2b37, Ugt1a6, Ugt2b, Cyp3a2 and Cyp2c13 in liver tissue. UDPGT[16] is important in the conjugation and subsequent elimination of potentially toxic xenobiotics and endogenous compounds, which catalyse the transfer of glucuronic acid from uridine diphosphoglucuronic acid to a variety of substrates, including steroid hormones. Ugt2b37 participates in the glucuronidation of testosterone and dihydrotestosterone, Ugt1a6 transforms small lipophilic molecules into water-soluble and excretable metabolites, Ugt2b conjugates lipophilic aglycon substrates with glucuronic acid;[17] thus, *R. Scrophulariae* may detoxify liver tissue. Cyp3a2 and Cyp2c13 are important drug metabolic enzymes in rat livers. Cyp3a2 activity was suppressed and appeared in cases of acute formaldehyde poisoning,[18] 5 week-old Zucker fatty diabetic rats,[19] and human immunodeficiency virus-infected rats.[20] One previous study has shown that CYP2C13 was absent in male hyperlipidaemic Sprague-Dawley rats.[21] However, *R. Scrophulariae* enhanced CYP2C13 levels in liver tissue, indicating that *R. Scrophulariae* may have protective effects.

However, down-regulation of carboxylic ester hydrolase and tyramine glucuronide by *R. Scrophulariae* may be toxic. Carboxylic ester hydrolase participates in phase I metabolism of xenobiotics such as toxins or drugs, and the resulting carboxylates are conjugated by other enzymes to increase solubility and are eventually excreted.[22] Tyramine glucuronide is a natural body metabolite of tyramine generated in the liver by UDP glucanosyltransferase.[23] Glucuronidation assists in excreting toxic substances, drugs and other substances that cannot be used as an energy source.[24] Glucuronic acid[25] attaches to the substance *via* a glycosidic bond, and the resulting glucuronide, which has a higher water solubility than the original substance, is eventually excreted by the kidneys. Therefore, further studies should be conducted on *R. Scrophulariae* toxicity.

R. Scrophulariae enhanced the level of Hsd17b2, which promotes the interconversion of estrone and oestradiol and regulates the biological activity of sex hormones.[26] Oestradiol is essential for reproductive and sexual functioning in women, and it also affects other organs including bones.[27] Thus, *R. Scrophulariae* may generate an oestrogen-like effect by raising Hsd17b2 levels. In addition, oestrogen assimilates protein in

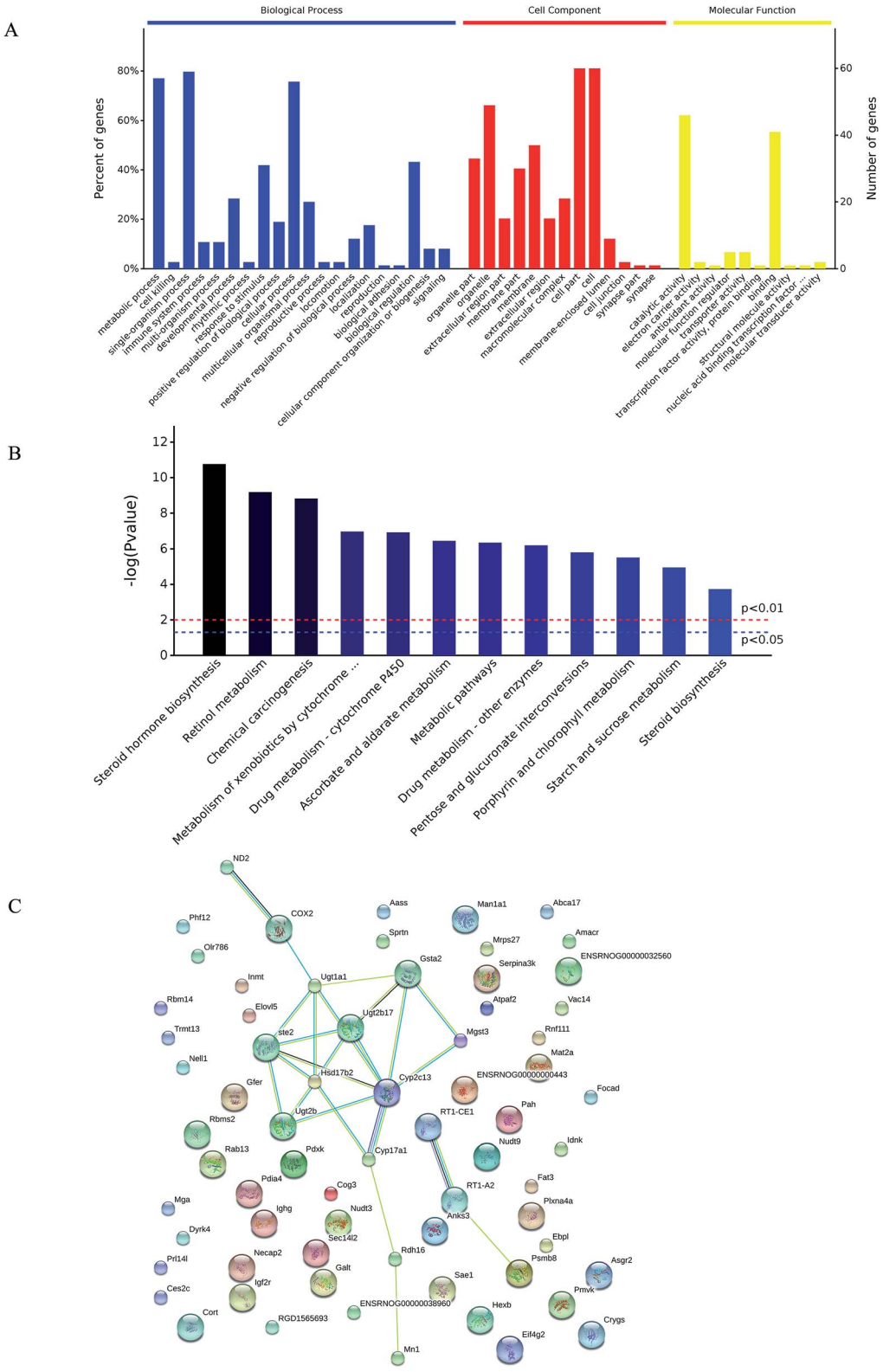

Fig. 3 Analysis of enriched gene ontology (A), KEGG pathway (B) and protein–protein interaction (C).

the liver and can also impact the male reproductive system, including androgen levels, causing testicular tissue structural changes and testicular cancer, reducing sperm counts, developing male breasts and leading to endocrine disorders.[28] Therefore, we must administer *R. Scrophulariae* appropriately to take advantage of its assimilation rather than its side effects.

In this study, Cyp17a1 and Gsta1 levels were increased by *R. Scrophulariae.* Cyp17a1 is a prominent inhibitory target in

treating prostate cancer because it produces the androgen required for tumour cell growth.[29] Studies found that Gsta1 was involved in metabolizing carcinogenic compounds.[30] These results may suggest that *R. Scrophulariae* has potential anti-cancer effects. In urine samples, *R. Scrophulariae* inhibited normorphine expression, a major metabolite of morphine. It acts directly on the central nervous system (CNS) to diminish sensations of pain.[31,32] The analgesic effect from *R. Scrophulariae* was minimal and likely related to the dosage.

R. Scrophulariae enhanced Gsta1 and Mgst3 expression in liver tissues. Gsta1 exhibits glutathione peroxidase activity, thereby protecting cells from reactive oxygen species and peroxidation products.[33] Mgst3 (microsomal glutathione s-transferase 3) is involved in the producing leukotrienes and prostaglandin E, important mediators of inflammation, and it demonstrates glutathione-dependent peroxidase activity towards lipid hydroperoxides.[34] Thus, *R. Scrophulariae* may produce antioxidant effects. However, it is worth noting that increases in serum and urinary Gsta1 have been found associated with hepatocyte and renal proximal tubular necrosis, respectively, and show potential for monitoring injury to these tissues.[35] *R. Scrophulariae* reduced isovalerylglucuronide expression. Elevated isovalerylglucuronide was reported in isovaleric acidaemia,[36] indicating that *R. Scrophulariae* may be used to treat isovaleric acidaemia by decreasing isovalerylglucuronide.

4 Conclusions

Untargeted urine metabolomics were performed by UPLC-TOF-MS, and proteomic liver profiling of *R. Scrophulariae*-treated rats was detected by nano-UPLC-Q- Exactive-MS/MS. We found that 5 common pathways were targeted by *R. Scrophulariae*, including steroid hormone biosynthesis, drug metabolism – cytochrome p450, drug metabolism – other enzymes, pentose and glucuronate interconversions, and starch and sucrose metabolism. These results show therapeutic effects as well as side effects. When administering *R. Scrophulariae* treatment, we should focus on its side effects. Curative effects of *R. Scrophulariae* included detoxification, anti-cancer, antioxidant and isovaleric acidaemia treatment. Since *R. Scrophulariae* was characterized by multiple targets and multiple pathways, finding the appropriate basis for its specific pharmacological effects is vital, as this process lays the foundation for clinically accurate and safe medication.

Conflicts of interest

There are no conflicts to declare.

References

1 C. C. Zhang, W. L. Gu, X. M. Wu, Y. M. Li, C. X. Chen and X. Y. Huang, Active components from Radix Scrophulariae inhibits the ventricular remodeling induced by hypertension in rats, *SpringerPlus*, 2016, **5**, 358, DOI: 10.1186/s40064-016-1985-z.

2 W. L. Gu, C. X. Chen, X. Y. Huang and J. P. Gao, The effect of angoroside C on pressure overload-induced ventricular remodeling in rats, *Phytomedicine*, 2015, **22**(7–8), 705–712, DOI: 10.1016/j.phymed.2015.05.002.

3 W. L. Gu, C. X. Chen, Q. Wu, J. Lu, Y. Liu and S. J. Zhang, Effects of Chinese herb medicine Radix Scrophulariae on ventricular remodeling, *Pharmazie*, 2010, **65**(10), 770–775.

4 X. Y. Huang, C. X. Chen, X. M. Zhang, Y. Liu, X. M. Wu and Y. M. Li, Effects of ethanolic extract from Radix Scrophulariae on ventricular remodeling in rats, *Phytomedicine*, 2012, **19**(3–4), 193–205, DOI: 10.1016/j.phymed.2011.09.079.

5 S. Y. Sheu, Y. W. Hong, J. S. Sun, M. H. Liu, C. Y. Chen and C. J. Ke, Radix Scrophulariae extracts (harpagoside) suppresses hypoxia-induced microglial activation and neurotoxicity, *BMC Complementary Altern. Med.*, 2015, **15**, 324, DOI: 10.1186/s12906-015-0842-x.

6 C. Chen, C. X. Chen, X. M. Wu, R. Wang and Y. M. Li, Effects of extracts of Radix Scrophulariae on blood pressure in spontaneously hypertensive rats and the underlying mechanisms, *Zhongxiyi Jiehe Xuebao*, 2012, **10**(9), 1009–1017.

7 X. Shen, T. Eichhorn, H. J. Greten and T. Efferth, Effects of Scrophularia ningpoensis Hemsl. on Inhibition of Proliferation, Apoptosis Induction and NF-kappaB Signaling of Immortalized and Cancer Cell Lines, *Pharmaceuticals*, 2012, **5**(2), 189–208, DOI: 10.3390/ph5020189.

8 Y. M. Li, Z. H. Han, S. H. Jiang, Y. Jiang, S. D. Yao and D. Y. Zhu, Fast repairing of oxidized OH radical adducts of dAMP and dGMP by phenylpropanoid glycosides from Scrophularia ningpoensis Hemsl, *Acta Pharmacol. Sin.*, 2000, **21**(12), 1125–1128.

9 X. Wang, A. Zhang, P. Wang, *et al.*, Metabolomics coupled with proteomics advancing drug discovery toward more agile development of targeted combination therapies, *Mol. Cell. Proteomics*, 2013, **12**(5), 1226–1238.

10 S. Qiu, A. Zhang, T. Zhang, *et al.*, Dissect new mechanistic insights for geniposide efficacy on the hepatoprotection using multiomics approach, *Oncotarget*, 2017, **8**(65), 108760–108770.

11 A. Zhang, X. Zhou, H. Zhao, *et al.*, Metabolomics and proteomics technologies to explore the herbal preparation affecting metabolic disorders using high resolution mass spectrometry, *Mol. BioSyst.*, 2017, **13**(2), 320–329.

12 H. Cao, A. Zhang, H. Sun, *et al.*, Metabolomics-proteomics profiles delineate metabolic changes in kidney fibrosis disease, *Proteomics*, 2015, **15**(21), 3699–3710.

13 X. Wang, A. Zhang, G. Yan, *et al.*, Metabolomics and proteomics annotate therapeutic properties of geniposide: targeting and regulating multiple perturbed pathways, *PLoS One*, 2013, **8**(8), e71403.

14 M. P. Thomas and B. V. Potter, The structural biology of oestrogen metabolism, *J. Steroid Biochem. Mol. Biol.*, 2013, **137**, 27–49, DOI: 10.1016/j.jsbmb.2012.12.014.

15 L. Yenush, J. M. Belles, J. M. Lopez-Coronado, R. Gil-Mascarell, R. Serrano and P. L. Rodriguez, A novel target of lithium therapy, *FEBS Lett.*, 2000, **467**(2–3), 321–325.

16 S. R. Salinas, A. A. Petruk, N. G. Brukman, M. I. Bianco, M. Jacobs, M. A. Marti, *et al.*, Binding of the substrate UDP-glucuronic acid induces conformational changes in the xanthan gum glucuronosyltransferase, *Protein Eng., Des. Sel.*, 2016, **29**(6), 197–207, DOI: 10.1093/protein/gzw007.
17 T. Izukawa, M. Nakajima, R. Fujiwara, H. Yamanaka, T. Fukami, M. Takamiya, *et al.*, Quantitative analysis of UDP-glucuronosyltransferase (UGT) 1A and UGT2B expression levels in human livers, *Drug Metab. Dispos.*, 2009, **37**(8), 1759–1768, DOI: 10.1124/dmd.109.027227.
18 M. Xu, H. Tang, Q. Rong, Y. Zhang, Y. Li, L. Zhao, *et al.*, The Effects of Formaldehyde on Cytochrome P450 Isoform Activity in Rats, *BioMed Res. Int.*, 2017, **2017**, 6525474, DOI: 10.1155/2017/6525474.
19 S. Y. Park, C. H. Kim, J. Y. Lee, J. S. Jeon, M. J. Kim, S. H. Chae, *et al.*, Hepatic expression of cytochrome P450 in Zucker diabetic fatty rats, *Food Chem. Toxicol.*, 2016, **96**, 244–253, DOI: 10.1016/j.fct.2016.08.010.
20 R. H. Ghoneim and M. Piquette-Miller, Endotoxin-Mediated Downregulation of Hepatic Drug Transporters in HIV-1 Transgenic Rats, *Drug Metab. Dispos.*, 2016, **44**(5), 709–719, DOI: 10.1124/dmd.115.067827.
21 P. J. Brassil, K. Debri, H. Nakura, S. Kobayashi, D. S. Davies and R. J. Edwards, Reduced hepatic expression of CYP7A1 and CYP2C13 in rats with spontaneous hyperlipidaemia, *Biochem. Pharmacol.*, 1998, **56**(2), 253–257.
22 Y. Chen, D. S. Black and P. J. Reilly, Carboxylic ester hydrolases: classification and database derived from their primary, secondary, and tertiary structures, *Protein Sci.*, 2016, **25**(11), 1942–1953, DOI: 10.1002/pro.3016.
23 K. P. Wong, The biosynthesis of tyramine glucuronide by liver microsomal fractions, *Biochem. J.*, 1977, **164**(3), 529–531.
24 H. Kaeferstein, Forensic relevance of glucuronidation in phase-II-metabolism of alcohols and drugs, *Leg. Med.*, 2009, **11**(suppl. 1), S22–S26, DOI: 10.1016/j.legalmed.2009.01.037.
25 S. S. Lewis, M. R. Hutchinson, Y. Zhang, D. K. Hund, S. F. Maier, K. C. Rice, *et al.*, Glucuronic acid and the ethanol metabolite ethyl-glucuronide cause toll-like receptor 4 activation and enhanced pain, *Brain, Behav., Immun.*, 2013, **30**, 24–32, DOI: 10.1016/j.bbi.2013.01.005.
26 E. Hilborn, O. Stal and A. Jansson, Estrogen and androgen-converting enzymes 17beta-hydroxysteroid dehydrogenase and their involvement in cancer: with a special focus on 17beta-hydroxysteroid dehydrogenase type 1, 2, and breast cancer, *Oncotarget*, 2017, **8**(18), 30552–30562, DOI: 10.18632/oncotarget.15547.
27 L. Tang, Z. Xia, Z. Luo, H. Long, Y. Zhu and S. Zhao, Low plasma PDGF-BB levels are associated with estradiol in postmenopausal osteoporosis, *J. Int. Med. Res.*, 2017, 300060517706630, DOI: 10.1177/0300060517706630.
28 K. M. Lau and K. F. To, Importance of Estrogenic Signaling and Its Mediated Receptors in Prostate Cancer, *Int. J. Mol. Sci.*, 2016, **17**(9), 1434.
29 S. N. Maity, M. A. Titus, R. Gyftaki, G. Wu, J. F. Lu, S. Ramachandran, *et al.*, Targeting of CYP17A1 Lyase by VT-464 Inhibits Adrenal and Intratumoral Androgen Biosynthesis and Tumor Growth of Castration Resistant Prostate Cancer, *Sci. Rep.*, 2016, **6**, 35354, DOI: 10.1038/srep35354.
30 C. Martinez-Guzman, P. Cortes-Reynosa, E. Perez-Salazar and G. Elizondo, Dexamethasone induces human glutathione S transferase alpha 1 (hGSTA1) expression through the activation of glucocorticoid receptor (hGR), *Toxicology*, 2017, **385**, 59–66, DOI: 10.1016/j.tox.2017.05.002.
31 P. A. Glare, T. D. Walsh and C. E. Pippenger, Normorphine, a neurotoxic metabolite?, *Lancet*, 1990, **335**(8691), 725–726.
32 H. Li, R. Tao, J. Wang and L. Xia, Upregulation of miR-375 level ameliorates morphine analgesic tolerance in mouse dorsal root ganglia by inhibiting the JAK2/STAT3 pathway, *J. Pain Res.*, 2017, **10**, 1279–1287, DOI: 10.2147/jpr.s125264.
33 L. G. Higgins and J. D. Hayes, Mechanisms of induction of cytosolic and microsomal glutathione transferase (GST) genes by xenobiotics and pro-inflammatory agents, *Drug Metab. Rev.*, 2011, **43**(2), 92–137, DOI: 10.3109/03602532.2011.567391.
34 F. P. Liu, X. Ma, M. M. Li, Z. Li, Q. Han, R. Li, *et al.*, Hepatoprotective effects of Solanum nigrum against ethanol-induced injury in primary hepatocytes and mice with analysis of glutathione S-transferase A1, *J. Chin. Med. Assoc.*, 2016, **79**(2), 65–71, DOI: 10.1016/j.jcma.2015.08.013.
35 V. Amlabu, C. Mulligan, N. Jele, A. Evans, D. Gray, H. J. Zar, *et al.*, Isoniazid/acetylisoniazid urine concentrations: markers of adherence to isoniazid preventive therapy in children, *Int. J. Tuberc. Lung Dis.*, 2014, **18**(5), 528–530, DOI: 10.5588/ijtld.13.0730.
36 L. Dorland, M. Duran, S. K. Wadman, A. Niederwieser, L. Bruinvis and D. Ketting, Isovalerylglucuronide, a new urinary metabolite in isovaleric acidemia. Identification problems due to rearrangement reactions, *Clin. Chim. Acta; international journal of clinical chemistry*, 1983, **134**(1–2), 77–83.

